



Published in final edited form as:

Mult Scler. 2012 April ; 18(4): 398–408. doi:10.1177/1352458512440060.

Protective effect of an elastase inhibitor in a neuromyelitis optica-like disease driven by a peptide of myelin oligodendroglial glycoprotein

Katja Herge¹, Brigit A de Jong², Ilan Kolkowitz¹, Caitlin Dunn¹, Gil Mandelbaum¹, Rose M Ko³, Alexander Maini¹, May H Han¹, Joep Killestein⁴, Chris Polman⁴, Alexandra L Goodyear¹, Jeffrey Dunn¹, Lawrence Steinman¹, and Robert C Axtell¹

¹Department of Neurology and Neurological Sciences, Stanford University, USA. ²Department of Neurology, Radboud University Nijmegen Medical Center, Nijmegen, The Netherlands.

³Department of Medicine, Division of Blood and Marrow Transplantation, Stanford University School of Medicine, USA. ⁴Department of Neurology, VU Medical Center, Amsterdam, The Netherlands.

Abstract

Background—The pathology of neuromyelitis optica (NMO), in contrast to multiple sclerosis, comprises granulocyte infiltrates along extensive lengths of spinal cord, as well as optic nerve. Furthermore, IFN- β treatment worsens NMO. We recently found that experimental autoimmune encephalomyelitis (EAE) induced with Th17 cells is exacerbated by IFN- β , in contrast to disease induced with Th1 where treatment attenuated symptoms.

Objective—This study demonstrates the similarities between NMO and Th17 EAE and how neutrophils mediate pathology in Th17 disease.

Methods—Levels of blood biomarkers in NMO were assessed by Luminex and ELISA. Effects of IFN- β on neutrophils were assessed by culture assays and immunofluorescence. EAE was induced by transfer of myelin-specific Th1 or Th17 cells and treated with Sivelestat sodium hydrate, a neutrophil elastase inhibitor.

Results—We show Th17 cytokines, granulocyte chemokines, type I interferon and neutrophil elastase are elevated in patients with definitive NMO. In culture, we find that IFN- β stimulates neutrophils to release neutrophil elastase. In Th17 EAE, we demonstrate neutrophilic infiltration in the optic nerve and spinal cord which was not present in Th1 EAE. Blockade of neutrophil elastase with Sivelestat had efficacy in Th17 EAE but not Th1 EAE.

Conclusions—The similarities between Th17 EAE and NMO indicate that this model represents several aspects of NMO. Neutrophils are critical in the pathologies of both Th17-EAE and NMO, and therefore blockade of neutrophil elastase is a promising target in treating NMO.

© The Author(s) 2012

Corresponding author(s): Robert C Axtell/Lawrence Steinman, Beckman Center B002, Department of Neurology, Stanford University, Stanford, California, 94305, USA. axterobe@stanford.edu or steinman@stanford.edu.

Conflict of interest

The authors declare no competing financial interests.

Keywords

multiple sclerosis; experimental autoimmune encephalomyelitis; Th17 cells; neutrophil elastase; neutrophil elastase inhibitor

Introduction

Neuromyelitis optica (NMO) and relapsing-remitting multiple sclerosis (RRMS) are both neuro-inflammatory diseases that lead to central nervous system (CNS) demyelination.¹ NMO is characterized by the presence of severe inflammation in the optic nerves and spinal cord,¹ and lesions are also found in the brain in 60–70% of patients.^{2,3} In addition, approximately 80% of patients with NMO develop auto-antibodies against Aquaporin 4 (AQP4), and the presence of AQP4-Ig is one clinical feature that is used to distinguish NMO from RRMS.⁴

One feature of the inflammatory cells that comprise NMO lesions is the presence of granulocytes, which are largely absent in RRMS lesions.¹ In NMO, IL-17 and IL-8 are elevated in the cerebrospinal fluid (CSF) compared with RRMS.^{5,6} In addition, the frequency of Th17 cells in the blood is elevated in NMO compared with RRMS.⁷ IL-17 signaling is known to upregulate chemokines that recruit and activate granulocytes, such as IL-8, G-CSF and Gro- α .^{8–10} The popular treatment for RRMS, beta-interferon (IFN- β), worsens NMO, increasing relapses and levels of AQP4 antibodies.^{11–14} We recently found that Th17-induced demyelination was exacerbated after IFN- β treatment.¹⁵ Overall, these data suggest that NMO is driven by the Th17 pathway, and that treatment with type 1 interferon exacerbates Th17-mediated disease.

In this study, we show that the signature of cytokines and chemokines and the cytopathology in the CNS are similar in patients with NMO and in mice with Th17-induced experimental autoimmune encephalomyelitis (EAE). We also demonstrate that inhibition of neutrophil elastase is effective in attenuating Th17-induced EAE. This finding implies that granulocyte enzymes are critical in the pathology of Th17 inflammatory CNS disease, and suggests that inhibition of neutrophil elastase could be a therapeutic strategy to treat acute relapses in NMO.

Methods

Clinical sample collection and blood analysis

Sixteen patients were diagnosed at the VU Medical Center in Amsterdam (VUMC) with NMO on or before 2006 and fulfilled the 1999 Wingerchuk criteria for NMO.¹⁶ All 16 patients had optic nerve and spinal cord inflammation, and none of the patients had brain magnetic resonance imaging (MRI) that fulfilled Barkhof/Tintore criteria for MS.^{17,18} Serum samples were obtained from these patients on a subsequent visit after diagnosis and were tested for the presence of NMO-Ig (Table 1). For comparison, sera from patients with definitive RRMS were also obtained from the VUMC (Supplementary Table). The study received approval from the Medical Ethics Board of the VUMC. In addition we obtained plasma samples from six patients with NMO which fulfilled the 2006 Wingerchuk criteria¹⁹ of NMO and seven healthy volunteers from the Stanford Multiple Sclerosis Center (Table 2). All subjects signed written informed consent.

We analyzed cytokines and chemokines in sera from NMO patients by multiplex bead analysis (Affymetrix). We analyzed neutrophil elastase in NMO and healthy plasma by enzyme-linked immunosorbent assay (ELISA) (eBioscience).

ELISA on cultured splenocytes

Splenocytes (0.5×10^6 cells/well) were cultured in flat-bottomed 96-well plates in media (RPMI 1640 supplemented with 2 mM 1-glutamine, 1 mM sodium pyruvate, 0.1 mM non-essential amino acids, 100 U/ml penicillin, 0.1 mg/ml streptomycin, 0.5 μ M 2-mercaptoethanol, and 10% FCS) with 5–20 μ g/ml MOG_{35–55} peptide for 3 days. Cytokines were measured in the supernatants of cultured cells using anti-mouse OPTIEIA ELISA kits for IL-2, IL-1 β , IL-5 and IFN- γ (BD Biosciences) and DuoSet kits for IL-17 and CXCL1 (R&D Systems).

T helper differentiation

We depleted spleen cells of CD8 T cells by magnetic sorting (Miltenyi) and stimulated the cells for 3 days with 1 μ g/ml of anti-CD3 (eBioscience) in non-polarizing, Th1 (10 ng/ml IL-12), Th17 (1 ng/ml rhTGF- β and 20 ng/ml rmIL-6), conditions in various concentrations of Sivelestat. Secretion of cytokines in the culture supernatants was assessed by ELISA.

Neutrophil extracellular trap assay

Neutrophils were isolated from whole blood of four healthy donors by lysis of red blood cells by ACK buffer and centrifugation through a Ficoll gradient. Neutrophil purity was assessed by fluorescence-activated cell sorting (FACS). Neutrophils were cultured on polylysine coverslips (BD Bioscience) for 4 h in media (RPMI 1640 supplemented with 2 mM 1-glutamine, 1 mM sodium pyruvate, 0.1 mM non-essential amino acids, 100 U/ml penicillin, 0.1 mg/ml streptomycin, 0.5 μ M 2-mercaptoethanol, and 10% FCS) with 10 U/ml rhIFN- β (R&D), 10 ng/ml C5a (R&D), both rhIFN- β and C5a or media only. Neutrophil extracellular trap (NET) release was assessed by fluorescent microscopy using DAPI staining, and antibodies to histone and neutrophil elastase adapted from Lin et al.²⁰ The number of NETs was counted in four visual fields per patient using ImageJ.

Experimental autoimmune encephalomyelitis

For adoptive transfer, female donor C57/BL6 mice were immunized via subcutaneous injection with 100 μ g MOG_{35–55} in an emulsion with complete Freund's adjuvant (CFA, Difco). Mice were also injected i.p. with 400 ng *Bordetella pertussis* toxin (List Biological Laboratories) at the time of and 2 days after immunization. Ten days after immunization spleen and draining lymph nodes were isolated and restimulated with 20 μ g/ml MOG_{35–55} in the presence of IL-12 (Th1) and IL-23 (Th17) for 3 days. Cytokines produced by both Th1 and Th17 cells were assessed by ELISA (Supplementary Figure 1). Female recipient C57BL/6 mice were injected i.p. with 50×10^6 cells.

Mice were examined daily for clinical signs of EAE and were scored on a five-point scale: 0, no clinical disease; 1, limp tail; 2, hind limb weakness; 3, complete hind limb paralysis; 4, hind limb paralysis plus some forelimb paralysis; and 5, moribund or dead. Animals were treated daily with 0.05 mg or 0.5 mg Sivelestat from day 6 to day 16 after transfer.

Animal protocols were approved by the Division of Comparative Medicine at Stanford University and animals were maintained in accordance with the guidelines of the National Institutes of Health.

Analysis of CNS-infiltrating cells

We isolated infiltrating cells from spinal cords or the brain-stem and cerebellum from three or four perfused mice. We incubated CNS homogenates with collagenase (Roche) and DNase (Sigma) for 1 h at 37°C and purified the cells by a Percoll gradient. FACS staining of CNS mononuclear cells was done using BD antibodies and protocols. Antibodies directed

against the following mouse cell-surface antigens were used: I-Ab, GR1, CD11b and CD4. In addition, intracellular staining of cytokines such as IFN- γ and IL-17 was performed. Data were acquired using a FACScan and analyzed by FlowJo software (Tree Star, Inc.). In addition, cells were cytopspun on glass slides and stained with Wright-Giemsa.

Histology

Brains and spinal cords were dissected from mice adoptively transferred with Th1 and Th17-differentiated cells and treated with Silvestat or PBS. Tissue was fixed in 10% formalin in PBS and embedded in a single paraffin block. Sections 8 μ m thick were stained with hematoxylin and eosin and luxol fast blue. The number of meningeal and parenchymal inflammatory foci was counted in 12 brain and spinal cord sections per mouse. Analysis of volume of infiltrated areas was performed with ImageJ.

Statistical analysis

Multiplex cytokine/chemokine data are presented as mean \pm the standard error of the mean (SEM). Significance was determined by a standard two-tailed Student's *t*-test. EAE data are presented as means \pm SEM, and we determined significance by a two-tailed Mann-Whitney test. ELISA, flow cytometry and histology data are presented as means \pm standard deviation (SD), and significance was determined by a two-tailed Student's *t*-test.

Results

Th17, granulocyte and interferon signatures are elevated in severe NMO

We obtained 16 serum samples from patients from the VUMC in Amsterdam (Table 1). At the time of blood draw all patients were in remission and five patients were on no medications, while the remainder of the cohort was on various immune modulators. At diagnosis, which was prior to the development of the revised Wingerchuk NMO criteria, all 16 patients fulfilled the 1999 Wingerchuk criteria¹⁶ based on clinical and brain and spinal cord MRI findings.^{17,18} The patients were later bled and tested for NMO-Ig. For analysis of the cytokine levels, the patients were divided into two groups:

1. Patients with contiguous spinal cords lesion extending three vertebral segments (*MRI*>*3seg*) and
2. Patients with spinal cord lesions less than three vertebral segments (*MRI*<*3seg*).

Four of the six *MRI*>*3seg* individuals were sera positive for NMO-Ig, whereas none were positive from the *MRI*<*3seg* group (Table 1). Using today's criteria for diagnosing NMO,¹⁹ the *MRI*>*3seg* patients were definitive NMO with more extensive myelopathic involvement than that of the *MRI*<*3seg* patients. The *MRI*<*3seg* patients are not definitively NMO by the Wingerchuk 2006 criteria.¹⁹

We compared levels of chemokines and cytokines in serum from these two groups of patients by Luminex multiplex bead assay. We observed elevated levels of both IL-17A and IL-17F in the *MRI*>*3seg* compared with the *MRI*<*3seg*, suggesting that the Th17 pathway is contributing to the disease (Figure 1 A, B). We also saw that there was an elevated neutrophil/granulocyte signature in NMO blood. The chemokine CXCL5 (ENA78), with an ELR motif, glutamic acid-leucine-arginine (ELR) immediately before the first cysteine of the CXC motif, and CXCL8 (IL-8)²¹ which are both potent chemo-attractants for neutrophils, were elevated in the serum of *MRI*>*3seg* patients (Figure 1C, D). We did not observe a difference in levels of IL-5, a cytokine implicated in the Th2/eosinophil pathway (Figure 1E). However, eotaxin 1, an eosinophil chemokine, was slightly but significantly elevated in the *MRI*>*3seg* group (Figure 1F).

IL-12p70, also known as IL-12, is a heterodimeric cytokine, comprising IL-12p40 and IL-12p35, and drives Th1 differentiation. IL-12p40 is a common subunit of both IL-12 and IL-23.²² We found that levels of IL-12p40 and IL-12p70 were not significantly different between the two groups (Figure 1G, H). IL-23 is implicated in the differentiation of Th17 cells,²³ and we anticipated that levels IL-23 would be elevated in NMO. This is currently under investigation.

We also observed that the individuals with $MRI > 3seg$ had elevated serum levels of the type I interferon IFN- β and the chemokine IP10 (Figure 1I, J), the expression of which is driven by type I IFN and type II IFN. This suggests that NMO, like systemic lupus erythematosus and psoriasis, has a type I IFN signature.^{24,25}

To verify that these definitive NMO patients ($MRI > 3seg$) were indeed different from MS patients, we compared levels of granulocyte chemokines from five of six of the definitive NMO ($MRI > 3seg$) serum samples with samples from 10 patients diagnosed with RRMS (see Supplementary Table). We found that patients with NMO had significantly elevated levels of CXCL5 and CXCL1 and a trend for elevated levels of CXCL8 compared with the patients with RRMS, suggesting that the Th17/granulocyte pathway is unique to patients with definitive NMO (Supplementary Figure 2).

Finally, we analyzed levels of neutrophil elastase in plasma from NMO spectrum patients (defined as being either NMO-Ig+ or having spinal cord lesions greater than three vertebral segments) compared with plasma from healthy volunteers (Table 2). Neutrophil elastase in blood can only be reliably tested in plasma, since neutrophils are activated in the processing of serum. Therefore, to make this measurement we obtained plasma from six patients with NMO and seven healthy volunteers from the Stanford Multiple Sclerosis Center (Table 2). We found that plasma from individuals with NMO spectrum diseases had elevated levels of neutrophil elastase compared with healthy controls (Figure 1K). These data demonstrate that neutrophils are activated in NMO, and this is highly suggestive that neutrophils play a major role in this disease.

Overall, these data indicate that patients with definitive NMO have a constellation of markers in their serum, which include signatures characteristic of a Th17 inflammatory condition, with granulocytic involvement driven by type I IFN.

Phenotypic comparison of Th17 and Th1-induced EAE

We recently reported that IFN- β treatment exacerbated EAE induced with Th17 cells but ameliorated EAE induced with Th1 cells.¹⁵ This worsening of disease with type 1 interferon is remarkably similar to the exacerbations seen after IFN- β treatment in patients with NMO.¹¹⁻¹⁴

To further demonstrate the similarity between Th17 EAE and NMO, we assessed the levels of cytokines and chemokines during Th1 and Th17-induced EAE. We induced EAE by transferring encephalitogenic T cells that were restimulated with MOG₃₅₋₅₅ peptide in the presence of IL-12 (Th1) or IL-23 (Th17) and analyzed the production of cytokines and chemokines by splenic T cells at the peak of EAE.

We found that IL-17, IL-5, and the ELR+ CXC chemokine CXCL1, which attracts neutrophils, were all significantly elevated in mice induced with Th17 EAE compared with Th1 EAE (Figure 2A). Conversely, there was a significantly increased production of IFN- γ in Th1 EAE compared with Th17 EAE (Figure 2A). Furthermore, there was no difference in the production of IL-2 by between Th1 and Th17-induced EAE (Figure 2A).

We next assessed the cellular composition of infiltrating CNS cells in Th1 and Th17-induced EAE at the peak of disease by flow cytometry analysis. As expected, we saw a predominant infiltration of IL-17-secreting cells in Th17-induced EAE and a predominance of IFN- γ -secreting cells in Th1-induced EAE (Figure 2B). Furthermore, mice with Th17 EAE had significantly more CD11b⁺/GR1^{hi}MHCII^{lo} cells in the CNS compared with Th1 EAE (Figure 2C, D). Conversely, mice with Th1-induced EAE had more CD11b⁺/GR1^{lo}MHCII^{hi} cells in the CNS compared with animals with Th17 EAE (Figure 2C, E). To confirm the identity of the infiltrating cells, we examined the morphology of the cellular infiltrate by cytopspin and Wright-Giemsa staining. We found that in Th17 EAE, infiltrating cells in the spinal cord were predominantly polymorphonuclear (PMN), which is a characteristic of neutrophils (Figure 2F). These PMNs were less prevalent in Th1 EAE spinal cords (Figure 2G).

The optic nerve and the spinal cord are preferentially affected in patients with NMO, whereas the cerebrum is mostly spared. In fact, we found that the optic tracts in Th17 EAE are heavily infiltrated compared with those in Th1 EAE (Figure 2H, I). Quantification showed that the percentage of lesion volume in optic tracts is 60% in Th17 EAE compared with 20% in Th1 EAE (Figure 2J). In addition, the predominant region of CNS infiltration in Th17 and Th1 EAE animals is in the spinal cord, whereas the cerebrum is much less infiltrated (Supplementary Figure 3A, B). This is somewhat contradictory to the report by Stromnes et al. which showed that EAE induced with Th17 has much more infiltration of the cerebrum than disease induced by Th1.²⁶ This discrepancy could be due to the differences in the strains used in the studies; we are using C57BL/6 whereas Stromnes et al. used the C3H strain. However, both of our studies demonstrate that immune-cell trafficking to the CNS differs between diseases induced with Th1 or Th17; we find predominantly more optic nerve infiltration in Th17 EAE compared with Th1 EAE.

In contrast to patients with MS, approximately 80% of patients with NMO have auto-antibodies to AQP4, which are deposited in lesions.⁴ When analyzing serum, we did not find that mice with Th17 EAE developed AQP4 antibodies (data not shown). However, IgG antibody staining of Th17 EAE lesions revealed large perivascular accumulations of antibodies in meningeal and parenchymal CNS lesions but not in non-inflamed tissue (Supplementary Figure 4A–C and E), which demonstrates that the blood-brain barrier is breached and suggests that auto-antibodies contribute to the pathology in this disease. We also found antibody deposition in the spinal cords of Th1 EAE, to a lesser extent, however, than the Th17 disease (Supplementary Figure 4D and E). The identity of the specificity of these antibodies is under investigation.

Type I IFN synergizes with complement to release neutrophil elastase from neutrophils

Since it is known that IFN- β exacerbates NMO symptoms and we previously found that IFN- β treatment worsens Th17 EAE, we questioned whether type I interferon has pro-inflammatory effects on neutrophils. Primary granules in neutrophils contain the proteolytic enzyme neutrophil elastase. This protease is highly destructive to tissues, and has been implicated in causing tissue damage in several inflammatory diseases including systemic inflammatory response syndrome (SIRS), cystic fibrosis, chronic obstructive pulmonary disease and lupus. One mechanism by which neutrophils cause tissue damage is through the release of NETs which contain histones, nuclear DNA and neutrophil elastase.²⁰ We cultured primary human neutrophils with media only, C5a only, IFN- β only, or both IFN- β and C5a together, and assessed the release of NETs by fluorescent microscopy. We found that both IFN- β and C5a alone marginally increase the formation of NETs compared with media alone. However, culturing neutrophils with both C5a and IFN- β significantly increased NET release compared with media only (Figure 3A, B).

Blockade of neutrophil elastase in Th1 and Th17 EAE

Overall, the data demonstrate that Th17 EAE models most aspects of the pathology of AQP4-Ig-negative NMO. Furthermore, these findings suggest that neutrophil recruitment and activity might have a pathogenic role in Th17 EAE but not in Th1 EAE, and their functional inhibition might be therapeutic in Th17 EAE and NMO.

To block neutrophil activity we used Sivelestat sodium hydrate, a selective inhibitor of neutrophil elastase.²⁷ Sivelestat is currently approved in Japan for the treatment of acute respiratory distress syndrome (ARDS) during SIRS.²⁸

C57BL/6 mice were adoptively transferred with pathogenic MOG-specific T cells that had been differentiated along either the Th1 or Th17 pathways. Animals were treated daily with 0.05 mg and 0.5 mg Sivelestat or vehicle control by daily intraperitoneal injections from day 6 until day 16 after transfer. We found considerable differences in the effect of Sivelestat treatment on EAE induced by Th1 and Th17 cells. Treatment with 0.5 mg Sivelestat significantly attenuated the progression of EAE in Th17-induced EAE (Figure 4A) but, in contrast, the clinical course of Th1-induced EAE was unchanged by Sivelestat treatment (Figure 4B). Furthermore, Sivelestat was found to have a dose-dependent effect in Th17 EAE, as treatment with 0.05 mg Sivelestat was less effective in reducing disease severity.

Histological analysis revealed that improved clinical status in mice with Th17 EAE treated with Sivelestat correlated with reduced inflammatory infiltrates in the spinal cord and the brain of Th17 EAE but not Th1 EAE (Figure 4C–E). We also found that Sivelestat reduced infiltration in the optic nerve in mice with Th17 EAE, which contrasts with the lack of treatment effect in Th1 EAE (Supplementary Figure 5). Furthermore, demyelination was reduced in Sivelestat-treated animals with Th17 EAE but not with Th1 EAE, compared with vehicle control (Figure 4F).

We also assessed the effect of Sivelestat treatment on splenic T cells isolated from mice with Th1 and Th17 EAE. In both Th1-induced and Th17-induced disease, IFN- γ , IL-1 β and CXCL1 production remained unchanged with Sivelestat treatment (Supplementary Figure 6). Accordingly, no treatment effect on CXCL1 production was seen in serum of animals (Supplementary Figure 7). However, Sivelestat had differential effects on IL-17, IL-2 and IL-5 in these disease models. In Th1-induced EAE, treatment with Sivelestat did not affect the production of IL-17 (Figure 4G) but, surprisingly, increased the production of IL-5 (Figure 4I). In Th17-induced EAE, IL-17 and IL-5 levels were lowered by Sivelestat treatment (Figure 4G, I). In both Th1 and Th17-induced disease, IL-2 production was equal. However, only in Th17 EAE did treatment with Sivelestat reduce the amount of IL-2 produced by splenic T cells (Figure 4H). Although absolute numbers of cytokine-producing cells infiltrating the spinal cord were significantly reduced in Sivelestat-treated Th17 EAE, we found no differences in the frequency of cytokine-producing CD4 T-cells (Supplementary Figure 8).

To directly test the effects of Sivelestat on T helper differentiation, we cultured spleen cells depleted of CD8 cells in Th1 and Th17 polarizing condition with various concentrations of Sivelestat or vehicle control. We found that Sivelestat had no significant effects on IL-17, IL-5 or IFN- γ production in these cultures (Supplementary Figure 9). This suggests that the effect Sivelestat had on these cytokines in EAE is not due to a direct effect on CD4 T cells or antigen-presenting cells.

Discussion

Since the discovery of the IL-23/Th17 pathway in EAE, much attention has understandably been focused on the role of Th17 in multiple sclerosis.^{29–31} However, our data, along with those of others, suggest that NMO is a Th17-driven demyelinating disease. In contrast, the majority of RRMS, except for a subset of IFN- β non-responders, may actually resemble a Th1-driven demyelinating disease.¹⁵ NMO lesions have an abundance of infiltrating granulocytes, containing both eosinophils and neutrophils, as opposed to what is seen in RRMS.¹ Our exploratory biomarker study now shows that sera from patients with definitive NMO contain elevated levels of the Th17 cytokines IL-17A and IL-17F, the neutrophil chemo-attractants CXCL5 and CXCL8, and the neutrophil protease, neutrophil elastase. Other studies have shown that IL-5 and other Th2 cytokines were elevated in the blood and CSF of patients with NMO. Surprisingly, in our NMO cohort we did not observe elevated levels IL-5, but we did see marginally elevated levels of eotaxin. Our serum biomarker study limits us from determining the specific cellular source of these cytokines. IL-17A and IL-17F are hallmark cytokines of Th17 cells,^{7,9,29} and a recent study suggests that T cells are the source of the elevated IL-17A in NMO compared with RRMS.⁷ However, these cytokines can be produced by many cell types including astrocytes, microglia and neutrophils, which add to the possible sources of IL-17 and related cytokines in NMO.^{32,33}

Type I IFN has an inflammatory role in NMO. Patients with NMO have exacerbations when treated with IFN- β , and we have found that IFN- β and IP10, which is a chemokine upregulated by type I and type II IFNs, are elevated the serum of patients with NMO. The mechanism by which type I IFN promotes symptoms in Th17-mediated autoimmunity is currently unknown. However, here we have demonstrated that type I IFN stimulates neutrophils to release neutrophil elastase through NET formation, and thus could contribute to the inflammatory effect of granulocytes in NMO.

The NMO phenotype has many features that are concordant with our observation with Th17-induced EAE. We previously demonstrated that IFN- β treatment exacerbated Th17 EAE. In the current study, we found that in Th17 EAE disease there are elevated levels of CXCL1, a strong chemo-attractant for neutrophils, and increased CNS-infiltrating neutrophils compared with Th1 EAE. Unexpectedly, we observed elevated IL-5 in Th17 EAE compared with Th1 EAE, another feature that has been previously reported in NMO. However, even with the elevated levels of IL-5, Th17 EAE did not reveal a significant amount of infiltrating eosinophils, which are seen in NMO lesions along with neutrophils.¹

B cells and auto-antibodies have been linked to the pathogenesis of NMO.⁴ Both rituximab and plasmapheresis treatments are showing promise as therapies for NMO. We found IgG deposition in the perivascular lesions in Th17 EAE, which demonstrates that the blood–brain barrier is breached but also suggests that auto-antibodies may play a major role in this disease pathway. It has been shown that 80% of patients with NMO have auto-antibodies to AQP4; this is a feature of this disease that distinguishes it from conventional MS.⁴ However, we did not find evidence that AQP4-Ig develop during the early stages of the Th17 EAE model. Astrocytosis is another clinical feature of NMO;¹ however, we did not observe the loss of astrocytes in the spinal cords of mice with Th17 EAE (data not shown).

Similar to the observation in NMO, Th17 EAE has an elevated level of a granulocyte-attracting chemokine CXCL1. Moreover, the CNS infiltrates are largely granulocytic. We found that blocking granulocyte activity, by inhibiting neutrophil elastase, attenuated the progression of clinical symptoms in mice with Th17 EAE but not Th1 EAE. In infectious conditions neutrophils are the first immune cells recruited to the site of inflammation, where they release serine proteases to eliminate microbes and then die quickly thereafter.³⁴ This

suggests that blocking neutrophil elastase with Sivelestat or another competitive elastase inhibitor might be a therapeutic strategy for the acute treatment of relapses in patients with NMO. Treatment with an elastase inhibitor could decrease the duration and dose of corticosteroid treatments, and in doing so eliminate some of the harmful effects of steroids.

Supplementary Material

Refer to Web version on PubMed Central for supplementary material.

Acknowledgments

Funding

This study was funded by the Guthy Jackson Foundation and US National Institutes of Health grant R01NS55997 to LS, a US National Institutes of Health grant 1K99NS075099-01 to RCA, and a Stanford school of medicine Dean's postdoctoral fellowship and German academic exchange program fellowship to KH.

References

1. Lucchinetti CF, Mandler RN, McGavern D, et al. A role for humoral mechanisms in the pathogenesis of Devic's neuromyelitis optica. *Brain*. 2002; 125(Pt 7):1450–1461. [PubMed: 12076996]
2. Nakashima I, Fujihara K, Miyazawa I, et al. Clinical and MRI features of Japanese patients with multiple sclerosis positive for NMO-IgG. *J Neurol Neurosurg Psychiatry*. 2006; 77(9):1073–1075. [PubMed: 16505005]
3. Pittock SJ, Weinshenker BG, Lucchinetti CF, et al. Neuromyelitis optica brain lesions localized at sites of high aquaporin 4 expression. *Arch Neurol*. 2006; 63:964–968. [PubMed: 16831965]
4. Paul F, Jarius S, Aktas O, et al. Antibody to aquaporin 4 in the diagnosis of neuromyelitis optica. *PLoS Med*. 2007; 4:e133. [PubMed: 17439296]
5. Ishizu T, Osoegawa M, Mei FJ, et al. Intrathecal activation of the IL-17/IL-8 axis in opticospinal multiple sclerosis. *Brain*. 2005; 128:988–1002. [PubMed: 15743872]
6. Uzawa A, Mori M, Arai K, et al. Cytokine and chemokine profiles in neuromyelitis optica: significance of interleukin-6. *Mult Scler*. 2010; 16:1443–1452. [PubMed: 20739337]
7. Wang HH, Dai YQ, Qiu W, et al. Interleukin-17-secreting T cells in neuromyelitis optica and multiple sclerosis during relapse. *J Clin Neurosci*. 2011; 18:1313–1317. [PubMed: 21795048]
8. Zhang Z, Zhong W, Spencer D, et al. Interleukin-17 causes neutrophil mediated inflammation in ovalbumin-induced uveitis in DO11.10 mice. *Cytokine*. 2009; 46:79–91. [PubMed: 19254849]
9. Liang SC, Long AJ, Bennett F, et al. An IL-17F/A heterodimer protein is produced by mouse Th17 cells and induces airway neutrophil recruitment. *J Immunol*. 2007; 179:7791–7799. [PubMed: 18025225]
10. Kroenke MA, Carlson TJ, Andjelkovic AV, Segal BM. IL-12- and IL-23-modulated T cells induce distinct types of EAE based on histology, CNS chemokine profile, and response to cytokine inhibition. *J Exp Med*. 2008; 205:1535–1541. [PubMed: 18573909]
11. Uzawa A, Mori M, Hayakawa S, et al. Different responses to interferon beta-1b treatment in patients with neuromyelitis optica and multiple sclerosis. *Eur J Neurol*. 2010; 17:672–676. [PubMed: 20039942]
12. Palace J, Leite MI, Nairne A, Vincent A. Interferon beta treatment in neuromyelitis optica: increase in relapses and aquaporin 4 antibody titers. *Arch Neurol*. 2010; 67:1016–1017. [PubMed: 20697055]
13. Shimizu J, Hatanaka Y, Hasegawa M, et al. IFN beta-1b may severely exacerbate Japanese optic-spinal MS in neuromyelitis optica spectrum. *Neurology*. 2010; 75:1423–1427. [PubMed: 20826711]
14. Warabi Y, Matsumoto Y, Hayashi H. Interferon beta-1b exacerbates multiple sclerosis with severe optic nerve and spinal cord demyelination. *J Neurol Sci*. 2007; 252:57–61. [PubMed: 17125797]

15. Axtell RC, de Jong BA, Boniface K, et al. T helper type 1 and 17 cells determine efficacy of interferon-beta in multiple sclerosis and experimental encephalomyelitis. *Nat Med*. 2010; 16:406–412. [PubMed: 20348925]
16. Wingerchuk DM, Hogancamp WF, O'Brien PC, Weinshenker BG. The clinical course of neuromyelitis optica (Devic's syndrome). *Neurology*. 1999; 53(5):1107–1114. [PubMed: 10496275]
17. Barkhof F, Filippi M, Miller DH, et al. Comparison of MRI criteria at first presentation to predict conversion to clinically definite multiple sclerosis. *Brain*. 1997; 120(11):2059–2069. [PubMed: 9397021]
18. Tintoré M, Rovira A, Martínez MJ, et al. Isolated demyelinating syndromes: comparison of different MR imaging criteria to predict conversion to clinically definite multiple sclerosis. *AJNR Am J Neuroradiol*. 2000 Apr; 21(4):702–706. [PubMed: 10782781]
19. Wingerchuk DM, Lennon VA, Pittock SJ, Lucchinetti CF, Weinshenker BG. Revised diagnostic criteria for neuromyelitis optica. *Neurology*. 2006; 66(10):1485–1489. [PubMed: 16717206]
20. Lin AM, Rubin CJ, Khandpur R, et al. Mast cells and neutrophils release IL-17 through extracellular trap formation in psoriasis. *J Immunol*. 2011; 187:490–500. [PubMed: 21606249]
21. Walz A, Burgener R, Car B, et al. Structure and neutrophil-activating properties of a novel inflammatory peptide (ENA-78) with homology to interleukin 8. *J Exp Med*. 1991; 174:1355–1362. [PubMed: 1744577]
22. Cua DJ, Sherlock J, Chen Y, et al. Interleukin-23 rather than interleukin-12 is the critical cytokine for autoimmune inflammation of the brain. *Nature*. 2003; 421:744–748. [PubMed: 12610626]
23. Langrish CL, Chen Y, Blumenschein WM, et al. IL-23 drives a pathogenic T cell population that induces autoimmune inflammation. *J Exp Med*. 2005; 201:233–240. [PubMed: 15657292]
24. Bennett L, Palucka AK, Arce E, et al. Interferon and granulopoiesis signatures in systemic lupus erythematosus blood. *J Exp Med*. 2003; 197:711–723. [PubMed: 12642603]
25. Nestle FO, Conrad C, Tun-Kyi A, et al. Plasmacytoid dendritic cells initiate psoriasis through interferon-alpha production. *J Exp Med*. 2005; 202:135–143. [PubMed: 15998792]
26. Stromnes IM, Cerretti LM, Liggitt D, et al. Differential regulation of central nervous system autoimmunity by T(H)1 and T(H)17 cells. *Nat Med*. 2008; 14(3):337–342. [PubMed: 18278054]
27. Kawabata K, Suzuki M, Sugitani M, et al. ONO-5046, a novel inhibitor of human neutrophil elastase. *Biochem Biophys Res Commun*. 1991; 177:814–820. [PubMed: 2049103]
28. Inoue Y, Tanaka H, Ogura H, et al. A neutrophil elastase inhibitor, Sivelestat, improves leukocyte deformability in patients with acute lung injury. *J Trauma*. 2006; 60:936–943. discussion 943. [PubMed: 16688053]
29. Durelli L, Conti L, Clerico M, et al. T-helper 17 cells expand in multiple sclerosis and are inhibited by interferon-beta. *Ann Neurol*. 2009; 65:499–509. [PubMed: 19475668]
30. Prinz M, Kalinke U. New lessons about old molecules: how type I interferons shape Th1/Th17-mediated autoimmunity in the CNS. *Trends Mol Med*. 2010; 16:379–386. [PubMed: 20591737]
31. Ramgolam VS, Sha Y, Jin J, et al. IFN-beta inhibits human Th17 cell differentiation. *J Immunol*. 2009; 183:5418–5427. [PubMed: 19783688]
32. Tzartos JS, Friese MA, Craner MJ, et al. Interleukin-17 production in central nervous system-infiltrating T cells and glial cells is associated with active disease in multiple sclerosis. *Am J Pathol*. 2009; 172:146–155. [PubMed: 18156204]
33. Werner JL, Gessner MA, Lilly LM, et al. Neutrophils produce interleukin 17A (IL-17A) in a dectin-1- and IL-23-dependent manner during invasive fungal infection. *Infect Immun*. 2011; 79:3966–3977. [PubMed: 21807912]
34. Borregaard N. Neutrophils, from marrow to microbes. *Immunity*. 2010; 33:657–670. [PubMed: 21094463]

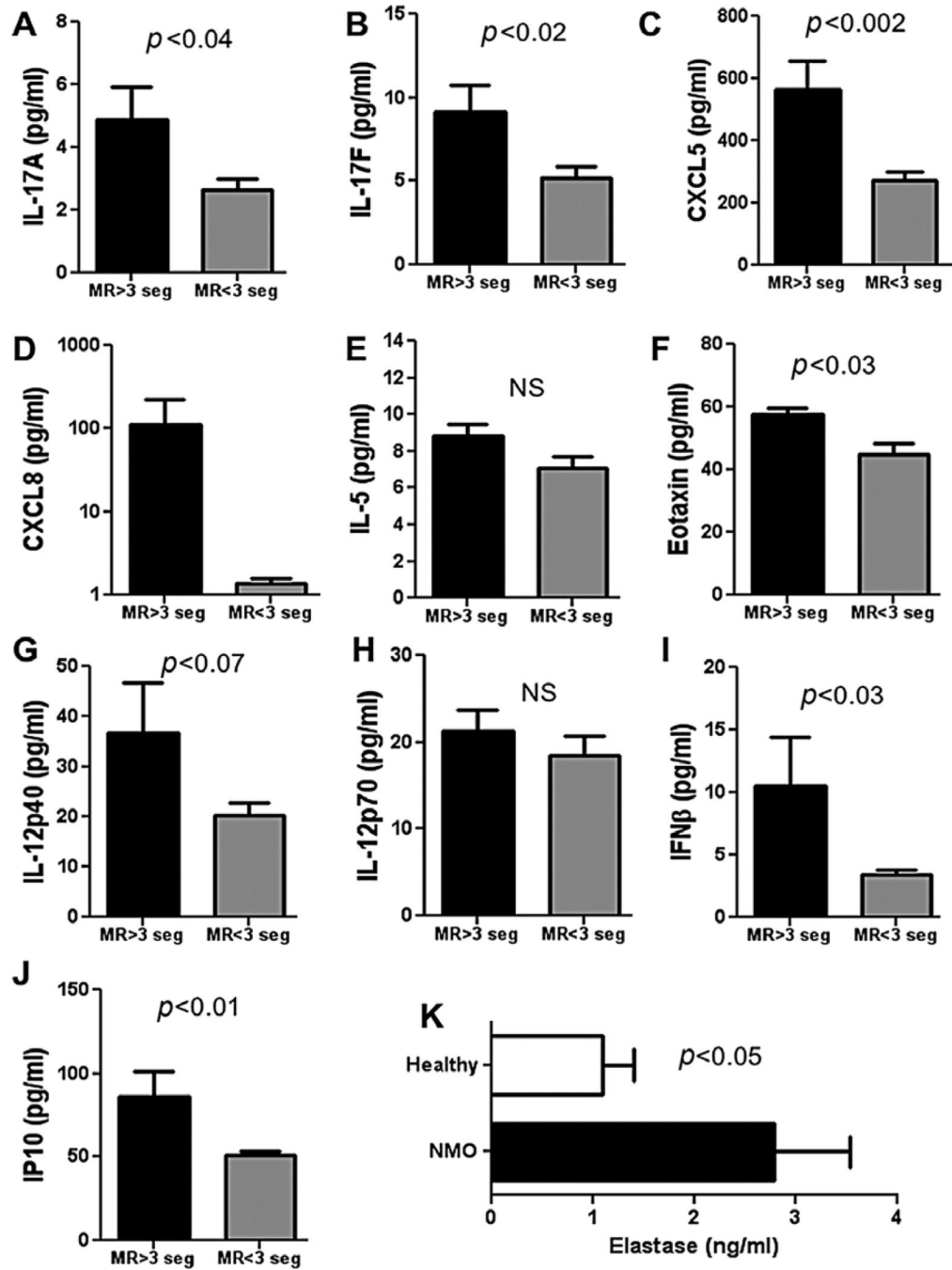


Figure 1. Blood biomarkers in patients with neuromyelitis optica

Concentration of IL-17A (A), IL-17F (B) CXCL5 (C), CXCL8 (D), IL-5 (E), Eotaxin I (F), IL-12p40 (G) and IL-12p70 (H) IFN-β (I), IP10 (J) in serum of six patients with Neuromyelitis optica (NMO) with spinal cord lesions greater than three vertebral segments ($MR > 3seg$) and 10 patients with NMO with spinal cord lesions less than three vertebral segments ($MR < 3seg$). Cytokine concentrations were measured by Luminex multiplex assay and calculated from a standard linear regression of known quantities of each cytokine. Neutrophil elastase (K) was measured in plasma from six NMO patients and seven healthy volunteers by ELISA. Data are represented as mean \pm SEM and p -values from two-tailed Student's t -tests are shown.

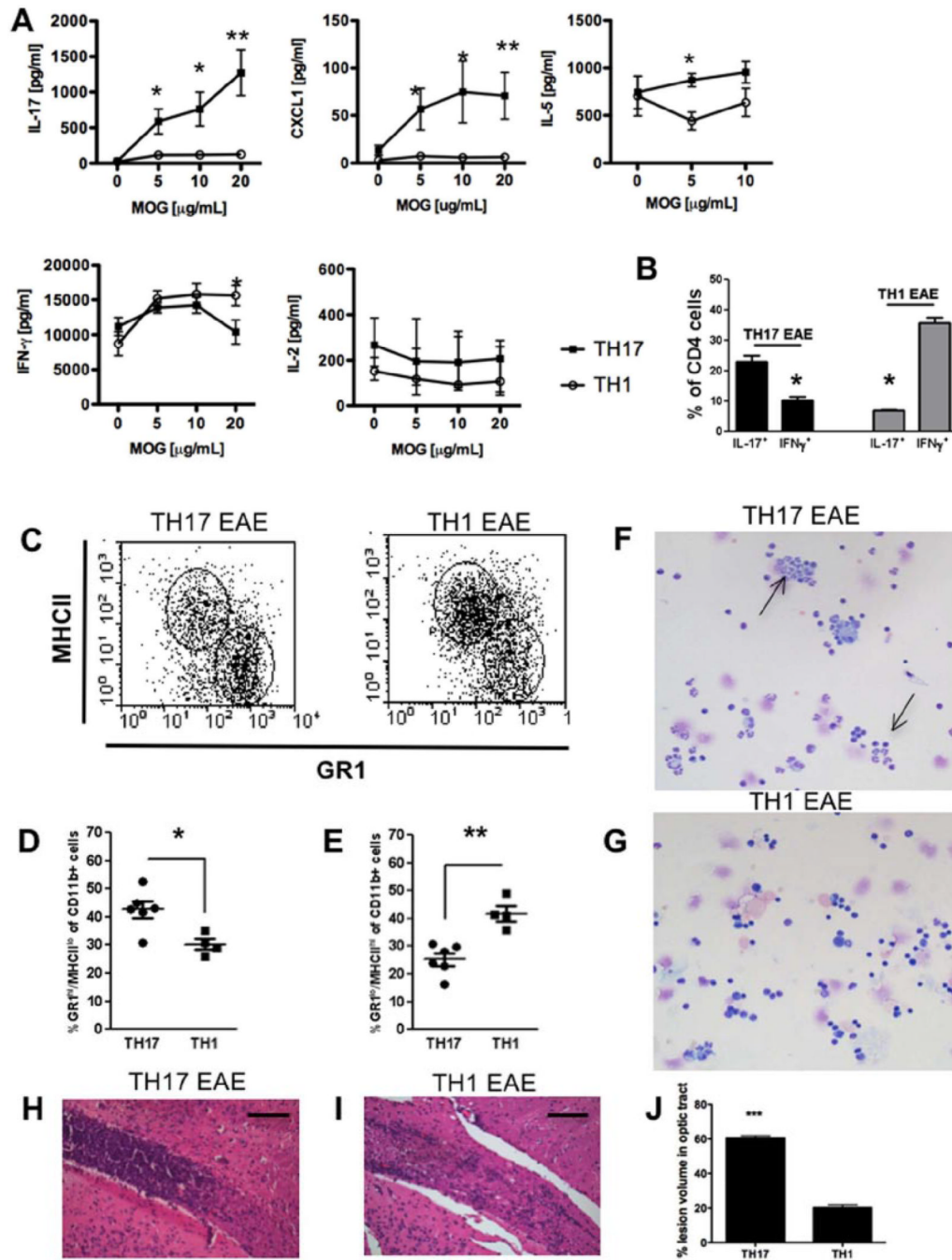


Figure 2. Phenotypic differences in Th17 and Th1-induced experimental autoimmune encephalomyelitis

To induce Th1 and Th17 experimental autoimmune encephalomyelitis (EAE), donor mice were sacrificed 10 days after MOG immunization (see methods) and spleens and draining lymph nodes were isolated and restimulated with 20 μg/ml MOG₃₅₋₅₅ in the presence of IL-12 (Th1) or IL-23 (Th17) for 3 days and transferred to healthy recipient mice to induce EAE. (A) Quantification of levels of IL-17, CXCL1, IL-5, IFN-γ and IL-2 in spleen culture supernatants of Th17 and Th1 EAE animals at peak of disease after 3 days of restimulation with MOG₃₅₋₅₅. Cytokine secretion was measured by ELISA. Results are shown as mean ±

SEM of three animals per group. IFN- γ : * $p < 0.04$; IL-17: * $p < 0.023$ ** $p < 0.005$; CXCL1: * $p < 0.039$ ** $p < 0.008$; IL-5: * $p < 0.026$.

(B) Flow cytometry analysis of IFN- γ and IL-17-secreting CD4⁺ cells from central nervous system (CNS) of Th17 and Th1-induced EAE mice at peak of disease. * $p < 0.05$.

(C–E) Flow cytometry analysis of MHCII⁺ and GR1⁺ cells of CD11b⁺ cells from CNS of Th17 and Th1-induced EAE mice at peak of disease (C). Quantification of GR1^{hi}MHCII^{lo}

(D) and GR1^{lo}MHCII^{hi} (E) cells of CD11b⁺ cells from CNS. Data represent individual values of 4–6 animals, mean and SEM. * $p < 0.03$, ** $p < 0.002$.

(F, G) Representative microphotographs of CNS infiltrates of Th17 (F) and Th1 (G) - induced EAE mice isolated by cytopspin. Cells were stained by Wright–Giemsa. Arrows show neutrophilic polymorphonuclear cells.

(H, I) Histology of inflammatory infiltrates in the optic tract of Th17 (H) and Th1 (I)- induced EAE stained with H&E at the peak of disease. Scale bars: 100 μ m.

(J) Quantification of lesion volume in optic tract of Th17 and Th1-induced EAE presented as percentage of lesion volume of the optic tract.

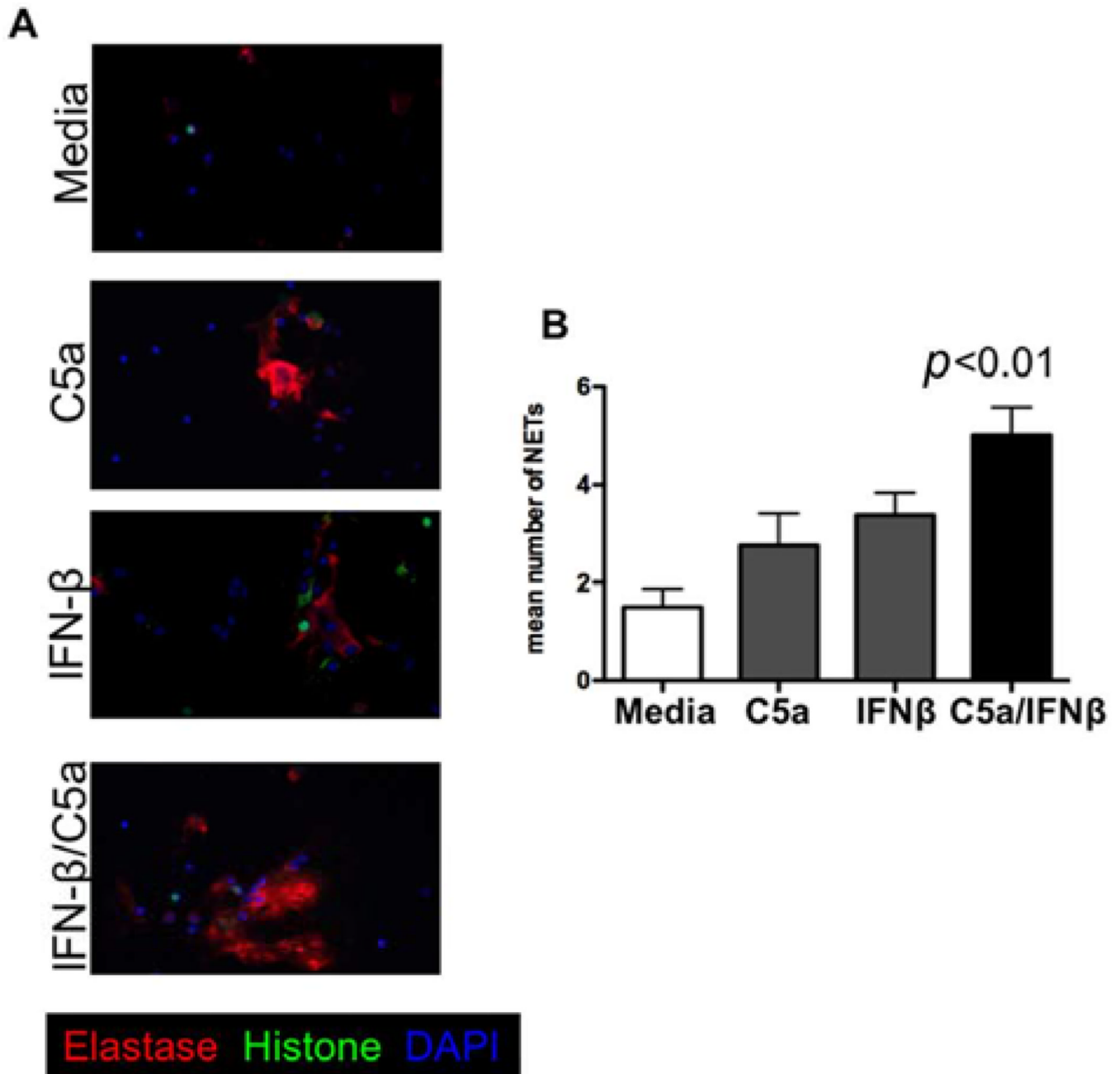


Figure 3. Type I IFN synergizes with complement to release neutrophil elastase from neutrophils (A) Representative immunofluorescence stainings of neutrophil elastase (red), histone (green) and DNA (blue) in human neutrophil cultures stimulated with media only, C5a, IFN- β and C5a + IFN- β for 4h. 20 \times . (B) Quantification of mean number of neutrophil extracellular traps (NETs) in neutrophil cultures of four healthy controls stimulated with media only, C5a, IFN- β and C5a + IFN- β . p -value from a two-tailed Student's t -test is shown.

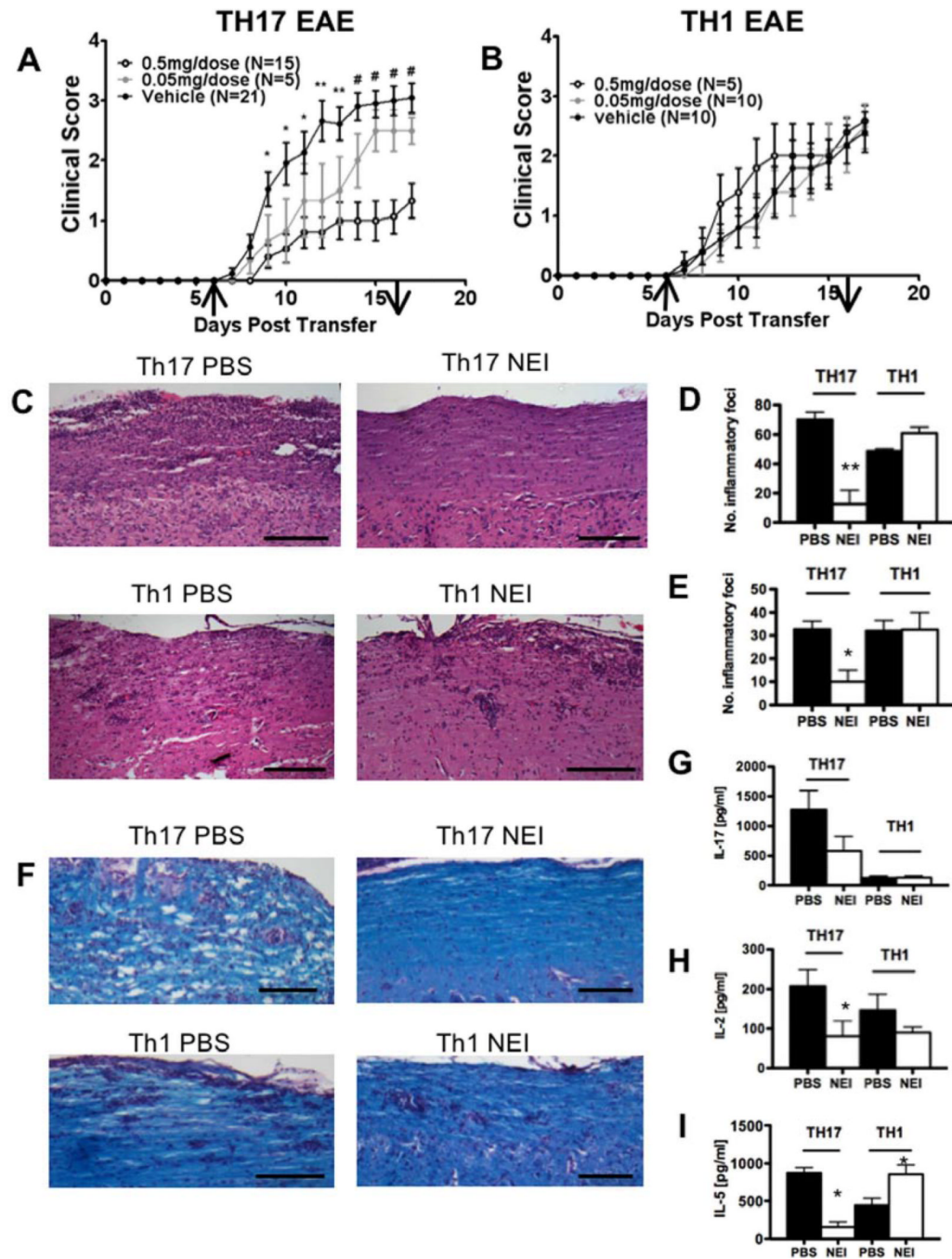


Figure 4. Sivelestat is effective in Th17 EAE but not in Th1 EAE

(A, B) Clinical scores from mice with passive experimental autoimmune encephalomyelitis (EAE) induced by adoptive transfer of Th17 (A) or Th1 (B) cells. Mice were treated with the indicated dose of Sivelestat or PBS i.p. every day from day 6 to 16 after transfer. Arrows depict initiation and termination of treatment. Results represent mean clinical score of 5–14 mice per group. Error bars represent means \pm SEM. * $p < 0.05$, ** $p < 0.01$, # $p < 0.005$. (C–F) Histology of spinal cord and brain sections from Th17- or Th1-induced EAE mice treated with Sivelestat or PBS. Sections of spinal cord and brain were obtained 9 days after transfer and stained with H&E (C) and Luxol fast blue (F). Scale bars: 100 μ m (C), 200 μ m (F). Quantification of number of inflammatory foci in spinal cord (D) and brain (E). Data

represent mean \pm SEM of three mice per group. * $p < 0.03$, ** $p < 0.009$. (G–I) Concentration of IL-17 (G), IL-2 (H) and IL-5 (I) from supernatants of MOG_{35–55}-stimulated spleen cells taken from mice 9 days after transfer of encephalitogenic Th17 or Th1 cells. Mice were treated with Silvestat or PBS starting at day 6. Data represent mean \pm SEM of three mice per group. * $p < 0.05$.

Table 1

Clinical and demographic features of serum specimens.

Patient	Sex	Age at diagnosis [years]	Diagnosis	Disease duration [years]	Treatment	Disease state	Spinal cord MRI	AQP-4 antibody
1	F	41	NMO	12	none	remission	MRI>3seg	positive
2	M	54	NMO	2	Azathioprine	remission	MRI>3seg	positive
3	F	25	NMO	15	Azathioprine	remission	MRI>3seg	positive
4	F	17	NMO	10	Copaxone	remission	MRI>3seg	positive
5	M	18	NMO	12	none	remission	MRI>3seg	negative
6	F	22	NMO	5	Rebif	remission	MRI>3seg	negative
7	F	39	NMO	5	Azathioprine	remission	MRI<3seg	negative
8	F	25	NMO	9	none	remission	MRI<3seg	negative
9	F	40	NMO	12	Azathioprine	remission	MRI<3seg	negative
10	M	31	NMO	12	none	remission	MRI<3seg	negative
11	F	40	NMO	9	Azathioprine	remission	MRI<3seg	negative
12	F	40	NMO	7	Methylprednisolone	remission	MRI<3seg	negative
13	F	33	NMO	13	Azathioprine	remission	MRI<3seg	negative
14	F	37	NMO	6	Azathioprine	remission	MRI<3seg	negative
15	F	30	NMO	4	unknown	remission	MRI<3seg	negative
16	F	36	NMO	12	none	remission	MRI<3seg	negative

* MRI>3seg: MRI revealed contiguous spinal cords lesion greater than three vertebral segments. MRI<3seg: MRI revealed spinal cord lesions less than three vertebral segments.

Table 2

Clinical and demographic features of plasma specimens.

Patient	Sex	Age at diagnosis [years]	Diagnosis	Disease duration [years]	Treatment	Length of treatment	Disease state	Spinal cord MRI*	AQP-4 antibody
1	F	49	NMO spectrum	<1	Rituximab	3 months	remission	MRI>3seg	positive
2	F	55	NMO spectrum	<1	Plasma exchange	1 cycle	remission	MRI>3seg	positive
3	M	24	NMO spectrum	<1	None		remission	MRI>3seg	negative
4	M	77	NMO	<1	Rituximab	1 month	remission	MRI<3seg	positive
5	F	59	NMO	1	None		remission	MRI>3seg	positive
6	F	25	NMO	2	Rituximab	twice yearly since 2009	remission	MRI>3seg	positive

* MRI>3seg: MRI revealed contiguous spinal cords lesion greater than three vertebral segments. MRI<3seg: MRI revealed spinal cord lesions less than three vertebral segments.